Subcortical correlates of consciousness with human single neuron recordings

Michael Pereira[1,2,3,*], Nathan Faivre[1,3*], Fosco Bernasconi[1,3,*], Nicholas Brandmeir[4], Jacob Suffridge[2,5], Kaylee Tran[2], Shuo Wang[2,5,6], Victor Finomore[2], Peter Konrad[4], Ali Rezai[2,4*], Olaf Blanke[1,7*]

Affiliations
1 Laboratory of Cognitive Neuroscience, Neuro-X Institute & Brain Mind Institute, Faculty of Life Sciences, Swiss Federal Institute of Technology (EPFL), Geneva 1202, Switzerland
2 Department of Neurosciences, WVU Rockefeller Neuroscience Institute, Morgantown, West Virginia
3 University Grenoble Alpes, University Savoie Mont Blanc, CNRS, LPNC, 38000 Grenoble, France
4 Departments of Neurosurgery, WVU Rockefeller Neuroscience Institute, Morgantown, West Virginia
5 Department of Computer Science and Electrical Engineering, West Virginia University, Morgantown, WV, 26506, USA
6 Department of Radiology, Washington University in St. Louis, St. Louis, MO, 63110, USA
7 Department of Clinical Neurosciences, University Hospital Geneva, Geneva, Switzerland
* equal contribution

Correspondence:
Michael Pereira
michael.pereira@univ-grenoble-alpes.fr
Laboratoire de Psychologie et Neurocognition
CNRS UMR 5105
UGA BSHM
1251 Avenue Centrale
38058 Grenoble Cedex 9
Twitter: @meaperei

Keywords: Neural correlates of consciousness, detection, deep brain stimulation, single neuron activity

Acknowledgments: MP was supported by two Postdoc.Mobility fellowships from the Swiss National Science Foundation (P2ELP3_187974; P400PM_199251). NF has received funding from the European Research Council (ERC) under the European Union's Horizon 2020 research and innovation program (grant agreement no. 803122). OB is supported by the Bertarelli Foundation, the Swiss National Science Foundation, and the European Science Foundation.

Author Contributions: MP, NF, FB, AR and OB developed the study concept and contributed to the study design. Neurosurgical procedures were carried out by NB, PK, and AR. Data collection was performed by MP, NF, FB, JS, and KT. Data analysis was carried out by MP, NF, FB. SW provided methodological support and VF supervised data collection. OB supervised the project. MP and NF drafted the paper; all authors provided critical revisions and approved the final version of the paper for submission.

Declaration of interest: The authors declare no competing interests.

Summary

Current methods to investigate the *neural correlates of consciousness* aim at contrasting the neural activity associated with different percepts under constant sensory stimulation to identify the minimal set of neuronal events sufficient for a specific conscious percept to occur (1–2). Much of this research has relied on subjective reports from humans to define conscious percepts (3), but only very few studies have found such contrasts at the single neuron level (4–8) and only in cortical regions of the human brain. The role of subcortical structures for perceptual consciousness is theoretically relevant (2,9,10) with some empirical support from detection studies in non-human primates (11,12), as well as functional imaging or local field potentials in humans (13,14). Nonetheless, it remains unknown whether and how the firing rate of subcortical neurons changes when a stimulus is consciously perceived. Here, we recorded individual neurons from the subthalamic nucleus (STN) and thalamus of human participants during 36 deep brain stimulation surgeries. While participants detected vibrotactile stimuli provided at the perceptual threshold, we found that neurons in both subcortical structures were modulated by the onset of the task or of the stimulus. Importantly, we found that 23% of the recorded neurons changed their activity when a stimulus was consciously perceived. Our results provide direct neurophysiological evidence of the involvement of subcortical structures in conscious detection with subjective reports, thereby calling for a less cortico-centric view of the neural correlates of consciousness.

Results

Task and behavior

Deep brain stimulation surgeries provide a unique opportunity to record the activity of single neurons in subcortical structures of the human brain. Microelectrode recordings are performed routinely after patients are awakened from anesthesia, to allow electrophysiologists and neurosurgeons to identify the target brain structure along the planned trajectory (Figures 1B, S1). During this procedure, we attached a vibrotactile stimulator to the palm of the hand contralateral to the microelectrode recordings and estimated the stimulus intensity corresponding to participants' individual tactile detection threshold. Once stable neuronal activity could be recorded in the target brain region (STN or thalamus), we proceeded to the main experiment, which comprised one or two sessions of 71 trials (total: 48 sessions). Each trial started with an audio "go" cue, followed by a vibrotactile stimulus applied at any time between 0.5 s and 2.5 s after the end of the cue (i.e. stimulation window), except for 20% of catch trials in which no stimulus was applied (Figure 1A). After a random delay ranging from 0.5 to 1 s, a "respond" cue was played, prompting participants to verbally report whether they felt a vibration or not. Therefore, none of the

reported analyses are confounded by motor responses. Using a staircase procedure, the stimulus intensity was kept around the detection threshold over the whole experiment. When possible, participants were trained to perform the task prior to the surgery.

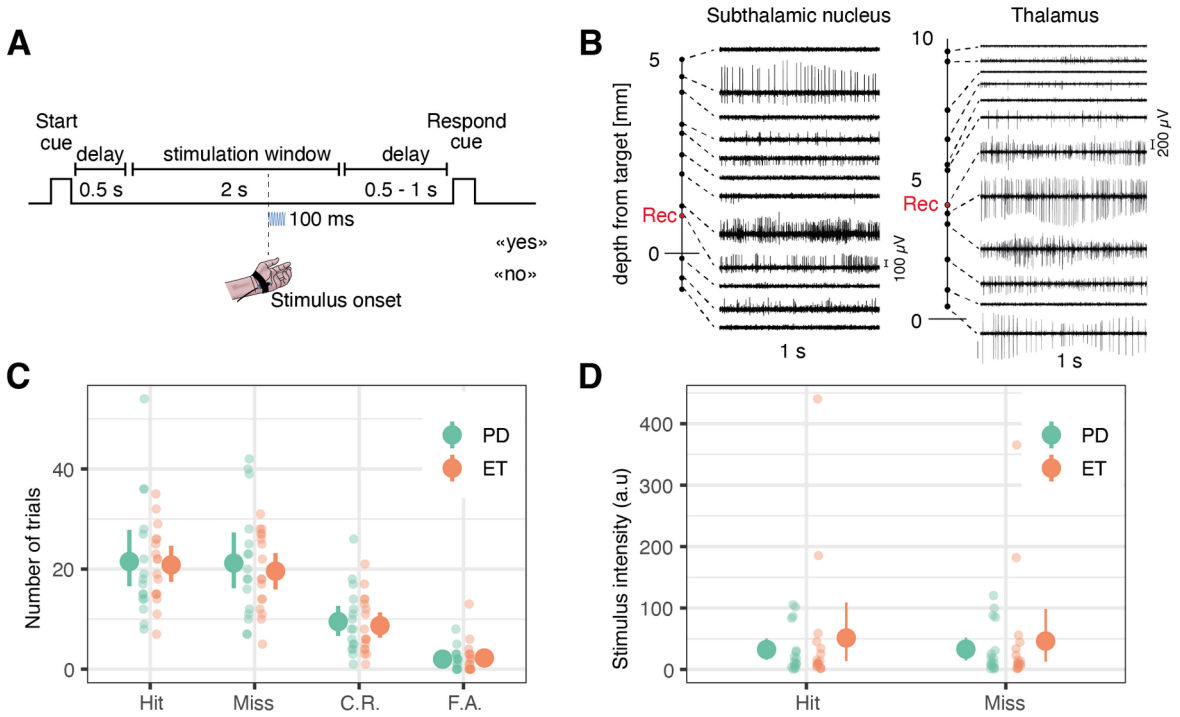

Figure 1. Task and behavior. A*. Task timeline. Each trial started with an auditory start cue, followed by a 0.5 s delay. Next, the stimulus could occur anytime during a 2 s stimulation window. After a variable 0.5 to 1 s delay, a response cue prompted patients to answer whether or not they detected the stimulus.* ***B****. Two example sets of 1 s long microelectrode recordings along the surgical tract showing specific firing for the subthalamic nucleus (left) and the motor thalamus (right). The depth at which the research data was collected is represented as a red dot (see Supplementary Figure 1 for anatomical correspondence).* ***C****. Number of hits, misses, correct rejections (C.R.), and false alarms (F.A.) collected during the main experiment.* ***D****. Averages of the absolute vibrotactile intensity in hits and misses in arbitrary units (values cannot be compared between participants). In panels C and D, each small dot represents a participant with Parkinson's Disease (PD, in green) or essential tremor (ET, in orange). Big dots represent averages; error bars represent 95% confidence intervals.*

When analyzing tactile perception, we ensured that our results were not contaminated with spurious behavior (e.g. fluctuation of attention and arousal due to the surgical procedure). We excluded specific series of trials from analyses based on objective criteria and focused on trials where hits and misses occurred in commensurate proportions (see methods). This procedure led us to keep 36 sessions out of 48 with a mean of 24.0 [95% confidence interval = 22.0, 25.9] hit trials and 22.7 [20.8, 24.5] miss trials. Permutation tests at the single-participant level indicated that detected and missed stimuli were of similar intensity except in 5 sessions for which the intensity of detected stimuli was higher on average. Likewise, detected and missed stimuli had similar onsets, except in 1 session for whom stimuli with

late onsets were predominantly missed, and in 2 sessions for whom stimuli with early onsets were predominantly missed. The hit rate was comparable between participants with Parkinson's disease (0.51 [0.49, 0.53]) and essential tremor (0.52 [0.51, 0.53], Wilcoxon rank sum test: W = 114.5, p = 0.45). Catch trials were separated into 9.1 [8.1 10.1] correct rejections and 2.1 [1.7, 2.6] false alarms, with an equivalent false alarm rate between participants with Parkinson's disease (0.24 [0.19, 0.28]) and essential tremor (0.24 [0.18, 0.30], Wilcoxon rank sum test: W = 145, p = 0.76). Intraoperative behavior was similar to the behavior observed during the training session and similar to what we found recently in a cohort of healthy participants using the same task (6).

Neuronal firing was modulated by the task

We performed a total of 48 (STN: 25, Thal: 23) successful microelectrode recording sessions during 36 surgeries for deep brain stimulation electrode implantation. We isolated 50 putative single neurons (STN: 26, Thal: 24) according to spike sorting metrics (Figure S2A-G). We ensured that all neurons showed stable spike amplitudes during the recording (Figure S2H-J). We also ensured that for every analysis, a minimum of 20 trials per condition were kept after removing artifacts. First, we looked for cue-selective neurons that modulate their firing rate during the 500 ms delay following the end of the "go" cue, compared to a 500 ms pre-cue baseline period. There were 8 / 44 (18 %) cue-selective neurons (Figure 2A; 6 neurons were removed from the analysis due to an insufficient number of trials). We confirmed that these 8 cue-selective neurons could not have been obtained by chance with permutation tests across neurons ($p < 0.001$). The proportion of cue-selective neurons was not significantly different in the STN (21%) and thalamus (15%; difference: $p = 0.31$, permutation test) and 6 out of 8 neurons showed a decrease in firing rate compared to the pre-cue baseline (Binomial test: $p = 0.145$).

Next, we investigated how many neurons showed task-selective modulations by comparing firing rates during the 2 s stimulation window to the 500 ms pre-cue baseline, indicating a modulation of their firing rate when a stimulus is expected. There were 9 / 44 (20 %) task-selective neurons ($p < 0.001$) with a similar proportion in the STN (20 %) and thalamus (21 %; $p = 0.91$; Figure 2B-D). Interestingly, 8 out of 9 neurons decreased their firing rate relative to the pre-cue baseline (Binomial test: $p = 0.020$). In both regions, a significant proportion (44 %; $p < 0.001$) of the task-selective neurons were also cue-selective, modulating their firing rate before any sensory stimulation necessary for a decision occurred. Therefore, these cue- and task-selective neurons are unlikely to be involved in decision-related action selection or cancellation (15,16) but should be involved in the detection task *per se*.

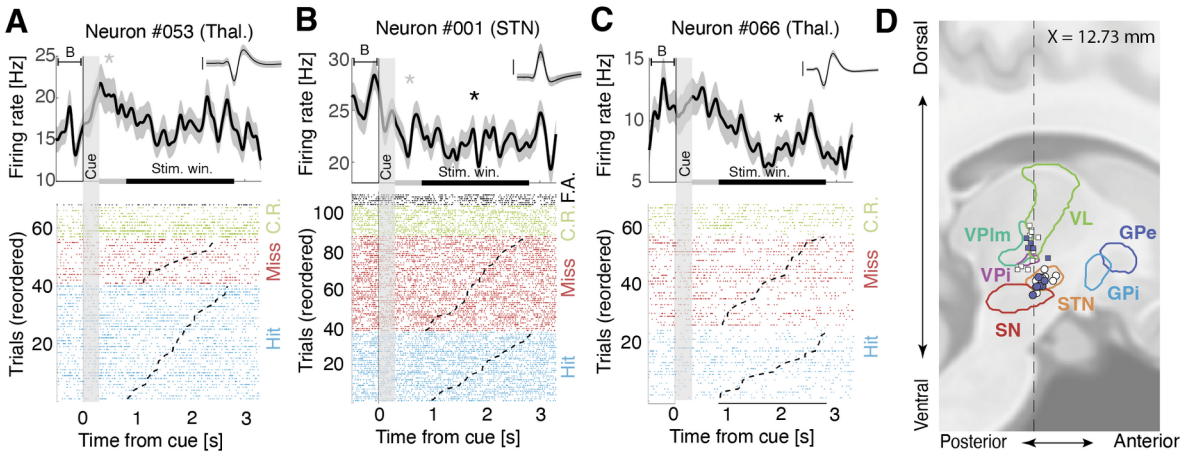

Figure 2. Representative cue- and task-responsive neurons in distinct patients. *Upper panels: firing rate time-locked to the onset of a trial (300 ms long auditory cue; vertical grey shade).* ***A-C****. Upper panels: firing rates during the task, compared to a 500 ms pre-cue baseline ("B"). Two significance windows were tested: the post-cue window (500 ms after cue offset; grey horizontal bar; cue-selective neurons) or the stimulation window (800 ms to 2800 ms post-cue; black horizontal bar; task-selective neurons). Asterisks represent statistical significance (p < 0.05). Shaded areas indicate bootstrapped standard errors. Inset: corresponding action potentials (shaded area indicates standard deviation; vertical bar corresponds to 100 µV). Lower panels: raster plot with trials sorted as hits (blue), misses (red), correct rejections (C.R.; green), and false alarms (F.A.; black).* ***A****. Cue-selective neuron in the thalamus.* ***B****. Cue- and task-selective neurons in the STN.* ***C****. Task-selective neuron in the thalamus.* ***D****. Sagittal view of recording locations for thalamic (squares) and subthalamic (circles) targets (see Figure S3A for a coronal view). Filled circles or squares are cue/task-selective neurons. Legend: VL: ventral lateral thalamus, VPlm: ventral posterior lateral and medial thalamus, VPi: ventral posterior inferior thalamus, STN: subthalamic nucleus, SN: substentia nigra, GPi/e: globus pallidus internalis / externalis,*

Neuronal firing was modulated by the stimulus

We then searched for neurons that modulate their firing rate after the stimulus onset compared to a 300 ms pre-stimulus baseline. We found 11 / 48 such stimulus-selective neurons (23%, p = 0.0020; Figure 3A-D; 2 neurons were removed due to an insufficient number of trials), with a similar proportion in the STN (21%) and in the thalamus (25%; difference: p = 0.807). These differences occurred 170 ms ± 30 after the stimulus onset, lasted for an average of 150 ms ± 20, and 9 out of 11 neurons showed a decrease in firing rate after the stimulus onset (p = 0.033). These results show that subthalamic and thalamic neurons are modulated by stimulus onset, irrespective of whether it was reported or not, even though no immediate motor response was required.

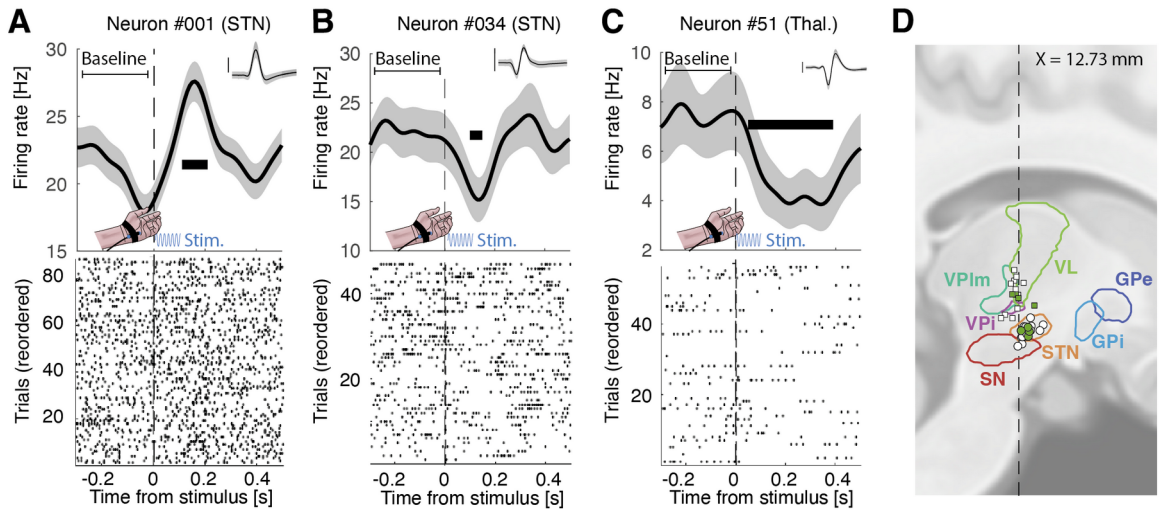

Figure 3. Representative stimulus-responsive neurons in distinct patients. A-C*. Upper panels: firing rate time-locked to the onset of the stimulus (100 ms vibrotactile stimulation; blue sinusoid) for all trials. Thick horizontal black segments show significant time windows. Shaded areas indicate bootstrapped standard errors. Inset: corresponding action potentials (shaded area indicates standard deviation; vertical bar corresponds to 100 µV). Lower panels: raster plot. The 300 ms pre-stimulus baseline was used only for statistics.* ***D****. Sagittal view of recording locations for thalamic (squares) and subthalamic (circles) targets (see Figure S3B for a coronal view). Filled circles or squares are sensory-selective neurons. Legend: VL: ventral lateral thalamus, VPlm: ventral posterior lateral and medial thalamus, VPi: ventral posterior inferior thalamus, STN: subthalamic nucleus, SN: substentia nigra, GPi/e: globus pallidus internalis / externalis,*

Neuronal firing was modulated by tactile perception

Having identified subcortical neurons that were cue-, task- or stimulus-selective, we next sought to assess the role of these structures in conscious detection by comparing firing rates time-locked to detected vs missed stimuli. Of the 50 neurons recorded, 35 were associated with periods of high-quality behavior, allowing us to assume tactile stimulation at the perceptual threshold. We found 8 neurons (23 %) showing a significant difference after stimulus onset ($p = 0.0020$; Figure 4A-D). The proportion of these perception-selective neurons was similar in the STN (27 %) and the thalamus (20 %; difference: $p = 0.529$). These differences in firing rates occurred 160 ms ± 30 after the stimulus onset and lasted for an average of 90 ms ± 10. We note that, 6 out of 8 neurons had higher firing rates for missed trials than hit trials, although this proportion was not significant ($p = 0.145$). None of the aforementioned neurons showed sustained differences between the highest and lowest stimulus amplitudes nor between early and late stimulus onset within the 2 s stimulus window (Figure S4). Our control analyses confirm that our results do not stem from slight differences in stimulus amplitudes due to the staircase procedure or spurious differences induced by the start or response cues. Qualitatively, we found very little overlap between task-, stimulus- and perception-selective neurons (Figure S5). This result suggests that

neurons in these two subcortical structures have mostly different functional roles. We also found no clear indication that neurons with a beta-band oscillatory component were more or less selective.

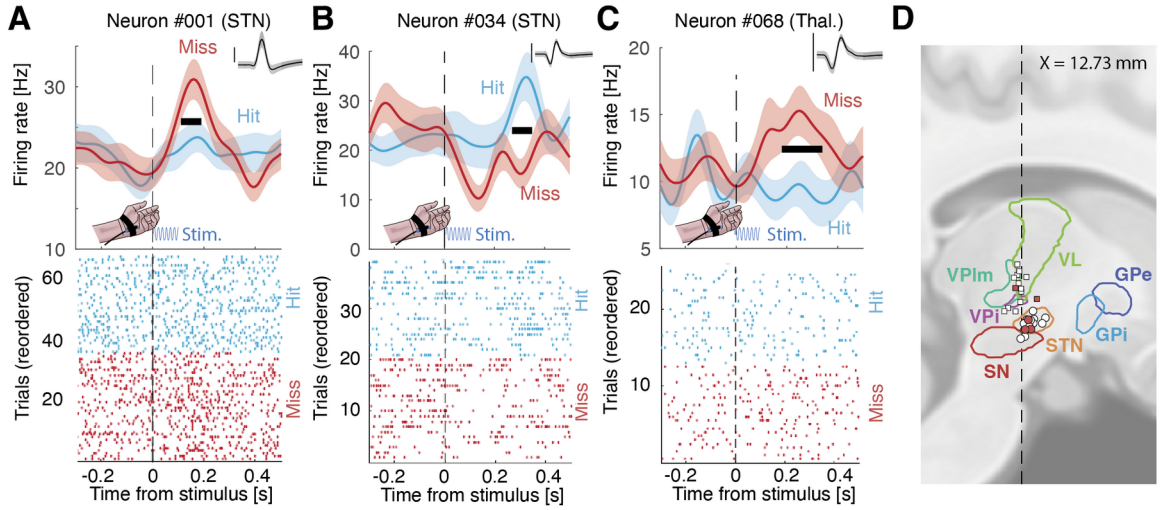

Figure 4. Representative perception-selective neurons in distinct patients. A-C *Upper panels: firing rate time-locked to the onset of the stimulus (100 ms vibrotactile stimulation; blue sinusoid) for hits (light blue) and misses (red). Thick horizontal black segments show significant time windows. Shaded areas indicate bootstrapped standard errors. Inset: corresponding action potentials (shaded area indicates standard deviation; vertical bar corresponds to 100 µV). Lower panels: raster plot for hits (light blue) and misses (red).* ***D****. Sagittal view of recording locations for thalamic (squares) and subthalamic (circles) targets (see Figure S3C for a coronal view). Filled circles or squares are perception-selective neurons. Legend: VL: ventral lateral thalamus, VPlm: ventral posterior lateral and medial thalamus, VPi: ventral posterior inferior thalamus, STN: subthalamic nucleus, SN: substentia GPi/e: globus pallidus internalis / externalis,*

Discussion

The role of subcortical structures in conscious detection with subjective reports is only rarely considered and poorly described, although their putative role for consciousness is largely acknowledged (2,9,10,17). This limit is likely due to the difficulty of recording subcortical activity in awake humans capable of providing conscious reports under controlled experimental conditions. We report the first intraoperative recordings of subcortical neurons in awake individuals providing conscious reports during a detection task. By imposing a delay between the end of the tactile stimulation window and the conscious report, we ensured that neuronal responses reflected conscious detection and not mere motor responses. In addition, because stimuli were applied on the palm, we asked participants to provide detection responses orally to avoid confounding neural activity related to sensory and motor processes of the upper limb. Our main result is that the activity of subcortical neurons co-varies with conscious reports following the presentation of detected vs missed

tactile stimuli. This result confirms that the neuronal underpinnings of conscious detection can be observed at the scale of single neurons (5–8) but also shows for the first time that they are not limited to the cortex.

Our findings that neurons in the thalamus modulate their activity according to conscious perception adds to the existing evidence in favor of the role of the thalamus during tactile detection. Indeed, thalamic activity and more precisely thalamocortical loops are often considered key to gate sensory stimuli to conscious access (10). In non-human primates, for example, oscillatory thalamic activity predicts tactile detection (11), and functional interactions between the somatosensory thalamus and the cortex increase when a tactile stimulus is detected (12). In humans, thalamic local field potentials and fMRI activity were higher for seen vs unseen stimuli (14) and causal effects of thalamic stimulation on the levels of consciousness have been found (18). Future studies with higher neuronal yields will be helpful in assessing the contribution of distinct thalamic territories to tactile consciousness, focusing notably on the ventral caudal part, which contains neurons with tactile receptive fields.

Concerning the subthalamic nucleus, a possibility is that perception-selective neurons determine conscious reports through the regulation of decisional processes involved when detecting a stimulus. Indeed, previous studies reported a modulatory role of subthalamic activity on decisional processes, notably by elevating the decisional threshold in conflict tasks (19–22). In a recent study in which we measured the activity of cortical neurons in a similar task, we showed that a specific decisional process called evidence accumulation is also at play during conscious detection (6). Based on this finding, we proposed that percepts fade in and out of consciousness when evidence accumulated by cortical neurons passes a given threshold (23). The present results, therefore, indicate that the contribution of subthalamic neurons to decisional processes is not limited to conflict tasks or motor planning, but may also regulate the threshold at which accumulated evidence gives rise to a conscious percept. Considering the inhibitory role of the subthalamic nucleus on the cortex (15), the fact that many of the perception-selective neurons we found had higher firing rate for misses than for hits suggests a role in elevating that threshold, similar to what is found in decision tasks manipulating conflict or cautiousness and requiring immediate responses (21,20,24,22). Thus, our results suggest that the STN plays an important role in a subcortical network gating conscious access, although it might not encode conscious content *per se* (25).

Apart from perception-selective neurons, we also found a distinct population of neurons in both the STN and thalamus that modulated their firing rate both after the cue and during the task, and therefore much before the stimulus onset. These neurons cannot be involved in

detection-related processes but could instead be involved in task switching (26). We also found neurons that modulated their firing rates after the stimulus onset, irrespective of detection. Our results should be taken with caution as they are based on a small number of neurons due to the high complexity of intraoperative recordings, and because the number of trials we could collect was not sufficient to test the computational mechanisms underlying the neuronal activity we recorded. Future studies combining cortical and subcortical recordings would be useful to consolidate these findings and investigate how subcortical regulation interacts with the cortex. For example, the 160 ms latency we observed post-stimulus corresponds to the onset of a putative cortical correlate of consciousness, the perceptual awareness negativity (27). We confirmed that our detection task was compatible with a contrastive analysis of consciousness in that it elicited a similar number of yes (detected stimuli or hit trials) and no responses (missed stimuli or miss trials), irrespective of stimulus intensity or stimulus onset. Nevertheless, it will be important in future studies to examine if similar subcortical responses are obtained when participants passively experience stimuli without the instruction to report them (i.e., no-report paradigms) (28).

In sum, our study provides neurophysiological evidence from single neurons in humans that subcortical structures play a significant role in conscious detection either by themselves (10) or through their numerous connections with the cortex (9). A comprehensive account of the neural correlates of consciousness should, therefore, not be cortico-centric but also consider subcortical contributions.

References

1. Koch C, Massimini M, Boly M, Tononi G. Neural correlates of consciousness: progress and problems. *Nat Rev Neurosci*. 2016;17(5):307-21.
2. Seth AK, Bayne T. Theories of consciousness. *Nat Rev Neurosci*. 2022;23(7):439-52.
3. Francken, J. C., Beerendonk, L., Molenaar, D., Fahrenfort, J. J., Kiverstein, J. D., Seth, A. K., & van Gaal, S. (2022). An academic survey on theoretical foundations, common assumptions and the current state of consciousness science. *Neuroscience of Consciousness*, *2022*(1)
4. Fried I, MacDonald KA, Wilson CL. Single Neuron Activity in Human Hippocampus and Amygdala during Recognition of Faces and Objects. *Neuron*. 1997;18(5):753-65.
5. Gelbard-Sagiv H, Mudrik L, Hill MR, Koch C, Fried I. Human single neuron activity precedes emergence of conscious perception. *Nat Commun*. 2018;9(1):2057.
6. Pereira M, Megevand P, Tan MX, Chang W, Wang S, Rezai A, et al. Evidence accumulation relates to perceptual consciousness and monitoring. *Nat Commun*. 2021;12(1):3261.
7. Quiroga RQ, Mukamel R, Isham EA, Malach R, Fried I. Human single-neuron responses at the threshold of conscious recognition. *Proc Natl Acad Sci*. 2008;105(9):3599-604.
8. Reber TP, Faber J, Niediek J, Boström J, Elger CE, Mormann F. Single-Neuron Correlates of Conscious Perception in the Human Medial Temporal Lobe. *Curr Biol.* 2017;27(19):2991-2998.e2.

9. Dehaene S, Changeux JP. Experimental and Theoretical Approaches to Conscious Processing. *Neuron*. 2011;70(2):200-27.
10. Ward LM. The thalamus: gateway to the mind: Gateway to the mind. *Wiley Interdiscip Rev Cogn Sci*. 2013;4(6):609-22.
11. Haegens S, Vazquez Y, Zainos A, Alvarez M, Jensen O, Romo R. Thalamocortical rhythms during a vibrotactile detection task. *Proc Natl Acad Sci*. 2014;111(17):E1797-805.
12. Tauste Campo A, Vázquez Y, Álvarez M, Zainos A, Rossi-Pool R, Deco G, et al. Feed-forward information and zero-lag synchronization in the sensory thalamocortical circuit are modulated during stimulus perception. *Proc Natl Acad Sci.* 2019;116(15):7513-22.
13. Levinson M, Podvalny E, Baete SH, He BJ. Cortical and subcortical signatures of conscious object recognition. *Nat Commun*. 2021;12(1):2930.
14. Kronemer SI, Aksen M, Ding JZ, Ryu JH, Xin Q, Ding Z, et al. Human visual consciousness involves large scale cortical and subcortical networks independent of task report and eye movement activity. *Nat Commun*. 2022;13(1):7342.
15. Mink JW. The Basal Ganglia: Focused Selection and Inhibition of Competing Motor Programs. *Prog Neurobiol*. 1996;50(4):381-425.
16. Mosher CP, Mamelak AN, Malekmohammadi M, Pouratian N, Rutishauser U. Distinct roles of dorsal and ventral subthalamic neurons in action selection and cancellation. *Neuron*. 2021;109(5):869-881.e6.
17. Schiff ND. Central Thalamic Contributions to Arousal Regulation and Neurological Disorders of Consciousness. *Ann N Y Acad Sci*. 2008;1129(1):105-18.
18. Schiff ND, Giacino JT, Kalmar K, Victor JD, Baker K, Gerber M, et al. Behavioural improvements with thalamic stimulation after severe traumatic brain injury. *Nature*. 2007;448(7153):600-3.
19. Bogacz R, Usher M, Zhang J, McClelland JL. Extending a Biologically Inspired Model of Choice: Multi-Alternatives, Nonlinearity and Value-Based Multidimensional Choice. Philos Trans Biol Sci. 2007;362(1485,):1655-70.
20. Cavanagh JF, Wiecki TV, Cohen MX, Figueroa CM, Samanta J, Sherman SJ, et al. Subthalamic nucleus stimulation reverses mediofrontal influence over decision threshold. *Nat Neurosci.* 2011;14(11):1462-7.
21. Frank MJ, Samanta J, Moustafa AA, Sherman SJ. Hold Your Horses: Impulsivity, Deep Brain Stimulation, and Medication in Parkinsonism. *Science*. 2007;318(5854):1309-12.
22. Herz DM, Zavala BA, Bogacz R, Brown P. Neural Correlates of Decision Thresholds in the Human Subthalamic Nucleus. *Curr Biol.* 2016;26(7):916-20.
23. Pereira M, Perrin D, Faivre N. A leaky evidence accumulation process for perceptual experience. *Trends Cogn Sci*. 2022;S1364661322000614.
24. Green N, Bogacz R, Huebl J, Beyer AK, Kühn AA, Heekeren HR. Reduction of Influence of Task Difficulty on Perceptual Decision Making by STN Deep Brain Stimulation. *Curr Biol*. 2013;23(17):1681-4.
25. Aru J, Bachmann T, Singer W, Melloni L. Distilling the neural correlates of consciousness. *Neurosci Biobehav Rev*. 2012;36(2):737-46.
26. Hikosaka O, Isoda M. Switching from automatic to controlled behavior: cortico-basal ganglia mechanisms. *Trends Cogn Sci*. 2010;14(4):154-61.
27. Dembski C, Koch C, Pitts M. Perceptual awareness negativity: a physiological correlate of sensory consciousness. *Trends Cogn Sci*. 2021;25(8):660-70.
28. Frässle S, Sommer J, Jansen A, Naber M, Einhauser W. Binocular Rivary: Frontal Activity Relates to Introspection and Action But Not to Perception. *J Neurosci*. 2014;34(5):1738-47.
29. Brainard, D. H. The Psychophysics Toolbox, *Spatial Vision* 1997;10:433-436.
30. Pelli, D. G. The VideoToolbox software for visual psychophysics: Transforming numbers into movies, *Spatial Vision* 1997;10:437-442.
31. Kleiner M, Brainard D, Pelli D, 2007, “What’s new in Psychtoolbox-3?” *Perception 36 ECVP Abstract Supplement*.
32. Levitt H. Transformed Up-Down Methods in Psychoacoustics. *J Acoust Soc Am*. 1971;49(2B):467-77.

33. Ilinsky, I., Horn, A., Paul-Gilloteaux, P., Gressens, P., Verney, C., and Kultas-Ilinsky, K. Human Motor Thalamus Reconstructed in 3D from Continuous Sagittal Sections with Identified Subcortical Afferent Territories. *ENeuro* 2018; 5(3):1–17
34. Team RC. R: A language and environment for statistical computing. Published online 2020.
35. Wickham H, Averick M, Bryan J, Chang W, McGowan LD, François R, Grolemund G, Hayes A, Henry L, Hester J, Kuhn M. Welcome to the Tidyverse. *Journal of open source software*. 2019 4(43):1686.
36. Wickham SR, Amarasekara NA, Bartonicek A, Conner TS. The big three health behaviors and mental health and well-being among young adults: a cross-sectional investigation of sleep, exercise, and diet. *Frontiers in Psychology*. 2020; 11:579205.
37. Rutishauser U, Schuman EM, Mamelak AN. Online detection and sorting of extracellularly recorded action potentials in human medial temporal lobe recordings, in vivo. *J Neurosci Methods*. 2006;154(1-2):204-24.
38. Maris, E., and Oostenveld, R. Nonparametric statistical testing of EEG- and MEG-data. *Journal of Neuroscience Methods*. 2007. 164, 177–190.

Methods

Participants

We recorded high impedance electrophysiological signals from microelectrodes inserted intraoperatively in the subthalamic nucleus of 32 participants with Parkinson disease or essential tremor undergoing deep brain stimulation electrode implantation surgeries (N = 36). For individuals with Parkinson's disease, the age at the time of the recording was 60.4 ± 2.7 years and the average UPDRS III score was 40.6 ± 3.0 prior to surgery and was reduced to 20.8 ± 2.8 after the surgery ($p = 0.0015$, $z = 3.18$). We also recorded intraoperatively in the thalamus of individuals with essential tremor undergoing deep brain stimulation surgeries. The age at the time of the recording was 68.9 ± 3.2 years and the average TETRA motor score was 20.1 ± 2.9 prior to surgery. The study was approved by the institutional review board of the West Virginia University Hospital (WVU02HSC17; #1709745061) and all participants provided written informed consent prior to any data collection.

Experimental procedure

Participants performed a tactile detection task programmed in Matlab using the Psychophysics toolbox (29,30,31). When possible, participants were trained a few days before the surgery (N = 18 / 36 surgeries). Participants sat in a reclining chair in a quiet room (training session) or were lying in the operating room (main session). Every trial started with a 300 ms long auditory "go" cue delivered through an external loudspeaker placed near the participants. Following the end of the go cue and a delay of 500 ms, a 100 ms vibrotactile stimulus could be delivered at any time during a two second stimulation window (i.e., uniform distribution between 0.8 and 2.8 s after the onset of the go cue; Figure 1A) on the lateral palm contralateral to the deep brain implant. Stimuli were applied using a MMC3 Haptuator vibrotactile device from TactileLabs Inc. (Montréal, Canada) driven by a 230 Hz sinusoid audio signal. Participants reported orally whether they felt the stimulus or not and whether they were confident in their answer or not after an auditory "respond" cue played one second after the end of the stimulation window. The participants responses could thus consist in "yes, sure", "yes, unsure", "no, sure" and "no, unsure". The task was stopped after two sessions of 71 trials, or before in case of discomfort or other clinical constraints. As –upon waking from anesthesia– most participants did not use both confidence levels, confidence data was not analyzed.

To keep the vibrotactile stimulus intensity around the detection threshold, we first conducted a rough threshold search by presenting a series of stimuli whose intensity decreased by steps of 5% until participants reported not feeling them anymore. Then we presented series of low intensity stimuli whose intensities increased by step of 5% until participants reported feeling them again. These procedures were repeated until the experimenter deemed the results satisfying. We took the average between the thresholds obtained during these procedures as a seed for the main task. During the main task, a 1up/1down adaptive staircase procedure (32) ensured that the intensity was kept around the perceptual threshold by increasing the intensity by 5% after miss trial and decreasing the intensity by 5% after a hit trial. Of note, the absolute stimulus intensity is not informative and cannot be

compared across patients and sessions, as it varied according to different factors (e.g. the length of the cable or the manner with which the tactile stimulator was strapped onto the palm).

Surgical procedure

STN or thalamus targets and trajectories were defined preoperatively using CranialSuite (Neurotargeting Inc., Nashville, US) based on MRI scans. Both targets were then defined with respect to the AC-PC (commissural) line using standard atlas-based methods and refined based on individual anatomy. The entry point was chosen approximately 2 to 3 cm from the midline and 1 cm anterior from the coronal suture and adjusted to individual anatomy in order to avoid traversing brain sulci, lateral ventricles or the medial bridging veins. Scalp incisions and burr-hole drilling were performed under local (lidocaine) and general (propofol) anesthesia and a microelectrode (FHC, Maine, US) was inserted through a guide cannula using a microdrive placed either on a Leksell frame (N = 13 surgeries) or a 3D printed mould (N = 23 surgeries).

Electrophysiology

Once the microelectrode reached the target brain structure (STN or thalamus), the speed of the microdrive was reduced and neuronal activity was streamed to a loudspeaker, allowing the electrophysiologist to verify the depth of the preplanned trajectory. The main research task was initiated when a neuron showed stable activity for a few tens of seconds and the anatomical localization was confirmed by the electrophysiologist. Recording depths were saved and used offline to define the anatomical localization (see Anatomical localization section). Electrophysiological data were recorded from the 5 mm tip of the microelectrode, referenced to the guide cannula and an adaptive line noise canceller was applied. Data were digitized either using a Guideline 4000 LP+ amplifier (FHC, Maine, US) at 30 kHz (N = 21 surgeries), or using a Guideline 5 amplifier (FHC, Maine, US) at 32 kHz and resampled offline to 30 kHz (N = 14 surgeries).

Anatomical localization

For 34 / 50 neurons, preoperative MRI and postoperative CT scans (co-registered in patient native space using CranialSuite) were available to precisely reconstruct surgical trajectories and recording locations (for the remaining 16 neurons, localizations were based on neurosurgical planning and confirmed by electrophysiological recordings at various depths). Recording depths were inspected along the trajectories in patient native space, projected to an MNI-coordinate space and compared against the Ilinsky atlas (33) which delineates distinct thalamic sub-territories based on a marker of γ-aminobutyric acid on sections post-mortem human brains (34).

Behavioral analyses

We used R 4.1.2 (34) and the tidyverse (35) and modelr (36) packages to analyze behavioral data. Permutation tests were performed by permuting hit and miss trials over 1000 iterations for each participant. Non-parametric p-values were estimated by counting the permutations for which the difference between hits and misses was higher in the observed compared to the shuffled data.

As titrating and keeping the vibrotactile stimulation intensity to the perceptual level after anesthesia was a challenging task, we took great care in keeping only the highest quality recordings. We estimated the trial-by-trial hit-rate using a sliding window of 11 trials (for the first and last 5 trials, we mirrored trials to avoid border effects). Any trial with a hit-rate out of the]25, 75[% range were removed from further analysis comparing hit to miss trials. If less than 10 hit and 10 miss trials were kept by this procedure, the session (and its corresponding neurons) was removed from subsequent analyses (13 / 48 sessions; 27 %).

Spike sorting and firing rate estimation

Each microelectrode recording was filtered between 300 and 3000 Hz and visually inspected. Artifacts such as cross-talk from the participants' vocal responses were marked and replaced by noise with a standard deviation matching the second pre- and post-artifact. We performed this procedure to avoid spuriously lowering the thresholds for neuronal spike detection. The timing of these artifactual epochs were saved in order to reject affected trials in later analyses. Neuronal spikes were detected and clustered using an online semi-automatic spike sorting algorithm (OSort) (37). Each resulting cluster of neurons was inspected based on common metrics such as spike waveform, percentage of inter-spike interval below 3 ms, signal-to-noise ratio and power spectral densities and possibly merged with other clusters. Finally, the resulting curated neurons were labeled as *putative single neuron* or *multiunit*, depending on the spike waveforms, peak amplitude distribution and the percentage of inter-spike interval below 3 ms. Electrophysiological signals were realigned either to the onset of the "go" cue (Figures 2) or to the onset of the stimulus (Figures 3-4), which was precisely obtained by applying a matched filter to a copy of the audio signal used to drive the vibrotactile stimulator we simultaneously recorded with the electrophysiological data. We estimated instantaneous firing rates using a sliding Gaussian kernel with a standard deviation of 40 ms and 1 ms steps. When displaying the resulting average firing rates over time, we estimated the standard error of the mean using a bootstrap procedure with 1000 resamplings.

Identification of selective neurons

To thoroughly control for false positives and possibly non-normal distributions, we exclusively used non-parametric statistics (Wilcoxon rank sum test, sign test), coupled with permutation tests. For each analysis, we verified that the reported number of neurons could not have been obtained by chance by comparing this number to a null distribution using permutation tests (38). For paired tests with respect to a baseline, we randomly flipped the sign of the difference between the firing rate during the trial and during the baseline and for unpaired tests, we randomly shuffled the conditions (i.e. a hit trial could be randomly assigned to a hit or a miss trial). To obtain a p-value, we compared the number of selective neurons to a null distribution obtained by randomly permuting the data 1000 times. This procedure allowed us to show that the number of selective neurons could not have been obtained by chance while controlling for multiple comparisons over time. Similarly, to test whether the proportion of neurons was different in the STN compared to the thalamus, we compared the absolute difference in the proportion of neurons in each anatomical location to a null distribution obtained by random permutations.

To identify cue-selective neurons we compared the number of spikes in a 500 ms baseline preceding the “go” cue to the number of spikes in a 500 ms period following the offset of the “go cue” using a two-tailed non-parametric sign test. Similarly, we identified task-responsive neurons by comparing the mean number of spikes in a 500 ms baseline preceding the “go” cue to the mean number of spikes during the 2 s stimulation window and performing a permutation test. We compared the differences in the proportion of selective neurons in the STN and thalamus, to the same differences observed in the shuffled data to assess its significance. Finally, we also compared the number of cue- and task-selective neurons to the same number observed in the shuffled data to assess whether the overlap was significant.

To identify detection-selective neurons, we looked for differences in the firing rates during the first 400 ms post-stimulus onset, assuming that subcortical signatures of stimulus detection ought to be found early following its onset. We defined a cluster as a set of adjacent time points for which the firing rates were significantly different between hits and misses, as assessed by a non-parametric Wilcoxon rank sum test. A putative neuron was considered perception-selective when the length of a cluster was above 80 ms, corresponding to twice the standard deviation of the smoothing kernel used to compute the firing rate. Whether for the shuffled data or the observed data, if more than one cluster was obtained, we discarded all but the longest cluster. This permutation test allowed us to control for multiple comparisons across time and participants.

Data and code availability

Data and code necessary to replicate our results are available online (https://gitlab.com/michael.pereira/subcortical-ncc).

Further information and requests should be directed to and will be fulfilled by the lead contact, Michael Pereira (michael.pereira@univ-grenoble-alpes.fr).